

See discussions, stats, and author profiles for this publication at: <https://www.researchgate.net/publication/244458775>

Syntheses and Reactivity of Heterometallic Oxo–Acetylide Cluster Compounds. Skeletal Rearrangement and Conversion of Acetylide to Alkenyl, Alkylidene, and Allenyl Ligands on a WRe...

ARTICLE *in* ORGANOMETALLICS · MAY 1997

Impact Factor: 4.13 · DOI: 10.1021/om9609426

CITATIONS

7

READS

14

6 AUTHORS, INCLUDING:



Yun Chi

National Tsing Hua University

344 PUBLICATIONS 10,830 CITATIONS

SEE PROFILE



Chi-Jung Su

Chung Shan Medical University

27 PUBLICATIONS 248 CITATIONS

SEE PROFILE

Syntheses and Reactivity of Heterometallic Oxo–Acetylide Cluster Compounds. Skeletal Rearrangement and Conversion of Acetylide to Alkenyl, Alkylidene, and Allenyl Ligands on a WRe₂ Framework

Yun Chi,^{*,†} Hsiao-Ling Wu,[†] Chi-Chung Chen,[†] Chi-Jung Su,[†]
Shie-Ming Peng,^{*,‡} and Gene-Hsiang Lee[‡]

Department of Chemistry, National Tsing Hua University, Hsinchu 30043, and Department of Chemistry and Instrumentation Center, National Taiwan University, Taipei 10764, Taiwan, Republic of China

Received November 5, 1996[®]

Oxidation of the mixed-metal cluster Cp^{*}WRe₂(CCR)(CO)₉ (**1**, Cp^{*} = C₅Me₅; R = Ph and C(Me)=CH₂) with dioxygen in solution at 100 °C affords the oxo clusters Cp^{*}W(O)Re₂(CCR)(CO)₈, (**2a**, R = Ph; and **2b**, R = C(Me)=CH₂). Treatment of **2** with CO at 110 °C provides the clusters Cp^{*}W(O)Re₂(CCR)(CO)₉ (**4**), which revert back to **2** by removal of one CO upon thermolysis. Both compounds **2** and **4** contain an open triangular skeletal arrangement, a multisite bound acetylide ligand, and a terminal oxo ligand attached to the W atom. Complex **2a** reacts with dihydrogen to form a mixture of three cluster complexes: the acetylide cluster Cp^{*}WRe₂(μ-O)(μ-H)₂(CCPh)(CO)₆ (**5a**), alkenyl cluster Cp^{*}W(O)Re₂(CHCHPh)(CO)₈ (**6a**), and the alkylidene cluster Cp^{*}W(O)Re₂(μ-H)(CHCH₂Ph)(CO)₈ (**7a**), which are formally produced by addition of two H₂ and elimination of two CO molecules, transferring one H₂ to the acetylide ligand and incorporation of one H₂ molecule to **6a**, respectively. For the vinylacetylide compound **2b**, it reacts with dihydrogen under similar conditions to furnish a mixture of the above mentioned clusters **5b**, **6b**, and **7b**, together with a fourth allenyl cluster Cp^{*}WRe₂(μ-O)(CHCCMe₂)(CO)₇ (**8**), which is probably produced through a 1,3-H-migration on the alkenyl ligand CH=CHC(Me)=CH₂ in **6b**. The X-ray structural analysis of these oxo cluster compounds, their spectroscopic data, and the mechanistic studies of the conversion from acetylide clusters **2**, **4**, and **5** to alkenyl clusters **6**, alkylidene clusters **7**, and allenyl cluster **8** are presented.

Introduction

Organometallic complexes containing oxo ligands serve as realistic models for metal-mediated oxidation and other homogeneous and heterogeneous reactions with high-valent metal species as catalysts.¹ As a result, a large number of oxo metal complexes have been synthesized; their reactivities with the organic substrates have been thoroughly explored.² The critical information obtained has helped chemists to understand the basic reaction pattern of the oxygen atom transfer reactions using discrete oxo complexes as catalysts.³ Another exploration is to synthesize complexes containing both oxo and hydrocarbyl ligands and to examine their chemistry, with the goal of probing the oxo ligand in promoting the various transformations on metal

complexes. The investigation of the reactivities of complexes MeReO₃, Re(O)H(C₂Et₂)₂, and (HB(pz)₃)ReO(Ph)Cl serve as typical examples of such an approach.⁴

With a goal of pursuing this research objective, we have first prepared a series of trinuclear mixed-metal acetylide cluster compounds with the empirical formula Cp^{*}WRe₂(CCR)(CO)₉ (**1**), where R = Ph, cyclohexenyl, and C(Me)=CH₂, and examined the chemical reactivity with H₂, alcohol, and thiophenol.⁵ Then, complexes **1** were subjected to oxidation by exposure to oxygen gas, which led to the successful isolation of oxo-containing acetylide cluster compounds Cp^{*}W(O)Re₂(CCR)(CO)₈ (**2**), R = Ph and C(Me)=CH₂, in high yield.⁶ The oxo complexes **2** have been shown to undergo fragmentation upon treatment with thiophenol in toluene to afford a

[†] National Tsing Hua University.

[‡] National Taiwan University.

[®] Abstract published in *Advance ACS Abstracts*, May 1, 1997.

(1) (a) Nugent, W. A.; Mayer, J. M. *Metal-Ligand Multiple Bonds*; Wiley-Interscience: New York, 1988. (b) Atagi, L. M.; Over, D. E.; McAlister, D. R.; Mayer, J. M. *J. Am. Chem. Soc.* **1991**, *113*, 870. (c) Dobbs, D. A.; Bergman, R. G. *J. Am. Chem. Soc.* **1993**, *115*, 3836. (d) Legzdins, P.; Phillips, E. C.; Rettig, S. J.; Trotter, J.; Veltheer, J. E.; Yee, V. C. *Organometallics* **1992**, *11*, 3104. (e) Rau, M. S.; Kertz, C. M.; Mercando, L. A.; Geoffroy, G. L.; Rheingold, A. L. *J. Am. Chem. Soc.* **1991**, *113*, 7420. (f) Schauer, C. K.; Voss, E. J.; Sabat, M.; Shriver, D. F. *J. Am. Chem. Soc.* **1989**, *111*, 7662.

(2) (a) Holm, R. H. *Chem. Rev.* **1987**, *87*, 1401. (b) Holm, R. H.; Donahue, J. P. *Polyhedron* **1993**, *12*, 571. (c) Woo, L. K. *Chem. Rev.* **1993**, *93*, 1125. (d) Dickman, M. H.; Pope, M. T. *Chem. Rev.* **1994**, *94*, 569.

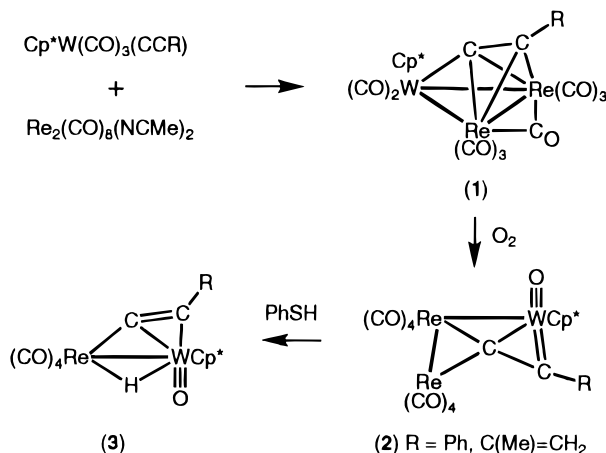
(3) (a) Clarke, R.; Gahagan, M.; Mackie, R. K.; Foster, D. F.; Cole-Hamilton, D. J.; Nicol, M.; Montford, A. W. *J. Chem. Soc., Dalton Trans.* **1995**, 1221. (b) Herrmann, W. A.; Fischer, R. W.; Rauch, M. U.; Scherer, W. *J. Mol. Catal.* **1994**, *86*, 243. (c) Herrmann, W. A. *J. Organomet. Chem.* **1995**, *500*, 149. (d) Herrmann, W. A.; Correia, J. D. G.; Kuehn, F. E.; Artus, G. R. J.; Romao, C. C. *Chem. Eur. J.* **1996**, *2*, 168. (e) Belgacem, J.; Kress, J.; Osborn, J. A. *J. Mol. Catal.* **1994**, *86*, 267.

(4) (a) Brown, S. N.; Mayer, J. M. *Organometallics* **1995**, *14*, 2951. (b) Herrmann, W. A.; Roesky, P. W.; Wang, M.; Scherer, W. *Organometallics* **1994**, *13*, 4531. (c) Cundari, T. R.; Conry, R. R.; Spaltenstein, E.; Critchlow, S. C.; Hall, K. A.; Tahmassebi, S. K.; Mayer, J. M. *Organometallics* **1994**, *13*, 322. (d) Tahmassebi, S. K.; Conry, R. R.; Mayer, J. M. *J. Am. Chem. Soc.* **1993**, *115*, 7553.

(5) Peng, J.-J.; Horng, K.-M.; Cheng, P.-S.; Chi, Y.; Peng, S.-M.; Lee, G.-H. *Organometallics* **1994**, *13*, 2365.

(6) Chi, Y.; Cheng, P.-S.; Wu, H.-L.; Hwang, D.-K.; Peng, S.-M.; Lee, G.-H. *J. Chem. Soc., Chem Commun.* **1994**, 1839.

Scheme 1



dinuclear complex $\text{Cp}^*\text{W}(\text{O})\text{Re}(\mu\text{-H})(\text{CCR})(\text{CO})_4$ (**3**) (Scheme 1),⁷ while the corresponding reactions of **1** with the same reagent only afforded the addition products, giving cluster compounds $\text{Cp}^*\text{WRe}_2(\mu_3\text{-Sph})(\text{CH}=\text{CPh})(\text{CO})_8$ and $\text{Cp}^*\text{WRe}_2(\mu_3\text{-Sph})(\text{CH}=\text{CPh})(\text{CO})_7$ as the final products.⁸ Such divergence in reactivity between **1** and **2** has provided the preliminary evidence about the potential influence of the oxo ligand on the chemical reactivities. In this study, we report the experimental results on the X-ray structural analyses and the reactivities of the W–Re oxo–acetylide complexes **2** toward CO and H₂, which offer an opportunity for further investigating this phenomenon.

Experimental Procedures

General Information and Materials. Infrared spectra were recorded on a Perkin Elmer 2000 FT-IR spectrometer. ¹H and ¹³C NMR spectra were recorded on a Bruker AM-400, a Varian Gemini-300 or a Varian Unity-400 instrument. Chemical shifts are quoted with respect to the internal standard tetramethylsilane (¹H and ¹³C NMR). Mass spectra were obtained on a JEOL-HX110 instrument operating in fast atom bombardment (FAB) mode. All reactions were performed under a nitrogen atmosphere using deoxygenated solvents dried with an appropriate reagent. Reactions were monitored by analytical thin-layer chromatography (5735 Kieselgel 60 F₂₅₄, E. Merck), and the products were separated on commercially available preparative TLC plates (Kieselgel 60 F₂₅₄, E. Merck). The metal acetylides $\text{Cp}^*\text{W}(\text{CO})_3(\text{CCR})$, R = Ph and C(Me)=CH₂, and the rhenium acetonitrile complex $\text{Re}_2(\text{CO})_8(\text{NCMe})_2$ were prepared according to literature procedures.⁹ The acetylide clusters $\text{Cp}^*\text{WRe}_2(\text{CCR})(\text{CO})_9$ (**1**) were obtained from the reaction of $\text{Cp}^*\text{W}(\text{CO})_3(\text{CCR})$ with $\text{Re}_2(\text{CO})_8(\text{NCMe})_2$ in toluene. Elemental analyses were performed at the NSC Regional Instrumentation Center at National Cheng Kung University, Tainan, Taiwan.

Synthesis of $\text{Cp}^*\text{W}(\text{O})\text{Re}_2(\text{CCPh})(\text{CO})_8$. To a 100 mL round-bottomed flask, $\text{Cp}^*\text{WRe}_2(\text{CCPh})(\text{CO})_9$ (**1a**, 352 mg, 0.337 mmol) was dissolved into a mixture of toluene (30 mL) and *n*-hexane (30 mL). The solution was then brought to reflux under oxygen, during which the temperature of the oil bath was kept at 100 °C to avoid over heating the reaction mixture. After 2.5 h, the color of the solution changed from orange-red to dark-red. The reaction was stopped, and the solvent was

evaporated. The residue was taken in CH₂Cl₂, separated by thin-layer chromatography (silica gel, dichloromethane:hexane = 1:1), and recrystallized from dichloromethane–methanol, giving 191 mg of $\text{Cp}^*\text{W}(\text{O})\text{Re}_2(\text{CCPh})(\text{CO})_8$ (**2a**) as dark-red crystalline materials (0.185 mmol, 64%), together with 53 mg of unreacted starting material. The vinylacetylide compound $\text{Cp}^*\text{W}(\text{O})\text{Re}_2[\text{CC}(\text{Me})=\text{CH}_2](\text{CO})_8$ (**2b**) was prepared under similar conditions in 48% yield.

Spectral data for **2a**: MS (FAB, ¹⁸⁴W, ¹⁸⁷Re) *m/z* 1034 (M⁺). IR C₆H₁₂ ν(CO): 2093 (m), 2060 (m), 2004 (vs), 1986 (s), 1979 (s), 1964 (w), 1958 (w), 1940 (vw) cm⁻¹. ¹H NMR (400 MHz, CDCl₃, 294 K): δ 7.43 (t, 2H, *J*_{HH} = 7.6 Hz), 7.37 (d, 1H, *J*_{HH} = 8.0 Hz), 7.30 (t, 2H, *J*_{HH} = 7.2 Hz), 2.00 (s, 15H, C₅Me₅). ¹³C NMR (100 MHz, CDCl₃, 294 K): CO, δ 198.3, 197.5, 197.1, 195.5, 191.9, 191.5, 189.8, 187.8; δ 211.4 (*J*_{WC} = 77 Hz, CPh), 184.6 (CCPh), 143.9 (1C, C₆H₅), 129.6 (2C, C₆H₅), 128.7 (1C, C₆H₅), 128.3 (2C, C₆H₅), 114.3 (C₅Me₅), 11.3 (C₅Me₅). Anal. Calcd for C₂₆H₂₀O₉Re₂W₁: C, 30.24; H, 1.95. Found: C, 30.00; H, 1.96.

Spectral data for **2b**: MS (FAB, ¹⁸⁴W, ¹⁸⁷Re) *m/z* 998 (M⁺). IR C₆H₁₂ ν(CO): 2091 (m), 2060 (m), 2003 (vs), 1986 (s), 1977 (s), 1964 (w), 1958 (w), 1937 (vw) cm⁻¹. ¹H NMR (400 MHz, CDCl₃, 294 K): δ 5.22 (s, 1H, *cis*-CH₂), 5.12 (s, 1H, *cis*-CH₂), 2.12 (s, 15H, C₅Me₅), 2.00 (s, 3H, Me). ¹³C NMR (100 MHz, CDCl₃, 294 K): CO, δ 198.4, 197.7, 197.3, 195.2, 192.3, 191.6, 190.6, 187.8; δ 212.8 (*J*_{WC} = 72 Hz, C_β), 181.9 (C_α), 149.1 (CMe=CH₂), 116.7 (CMe=CH₂), 114.1 (C₅Me₅), 23.3 (Me), 11.1 (C₅Me₅). Anal. Calcd for C₂₃H₂₀O₉Re₂W₁: C, 27.72; H, 2.02. Found: C, 27.52; H, 2.01.

Treatment of **2a with CO.** To a 300 mL thick-walled glass bottle, the toluene solution (60 mL) of **2a** (230 mg, 0.223 mmol) was heated at 90 °C under a CO atmosphere (3 atm) for 2 h during which the color changed from red to orange. The solvent was evaporated, and the residue was dissolved in CH₂Cl₂ and separated by thin-layer chromatography (dichloromethane:hexane = 1:2), giving 225 mg of $\text{Cp}^*\text{W}(\text{O})\text{Re}_2(\text{CCPh})(\text{CO})_9$ (**4a**, 0.212 mmol, 95%). Crystals of **4a** suitable for X-ray diffraction study were obtained from dichloromethane and heptane at room temperature. The vinylacetylide complex $\text{Cp}^*\text{W}(\text{O})\text{Re}_2[\text{CC}(\text{Me})=\text{CH}_2](\text{CO})_9$ (**4b**) was prepared under similar conditions.

Spectral data for **4a**: MS (FAB, ¹⁸⁴W, ¹⁸⁷Re) *m/z* 1062 (M⁺). IR C₆H₁₂ ν(CO): 2110 (s), 2052 (m), 2032 (vw), 2014 (vs), 2004 (vs), 1990 (w), 1976 (s), 1966 (w), 1811 (vw, br) cm⁻¹. IR (KBr) ν(W=O): 930 (br) cm⁻¹. ¹H NMR (300 MHz, CDCl₃, 294 K): δ 7.72 (d, *J*_{HH} = 7.5 Hz, 2H), 7.50 (t, *J*_{HH} = 7.5 Hz, 2H), 7.41 (t, *J*_{HH} = 7.5 Hz, 1H), 1.92 (s, 15H, Cp*). ¹³C NMR (100.6 MHz, CDCl₃, 294 K): CO, δ 226.0 (*J*_{WC} = 46 Hz, 1C), 194.5 (1C), 192.1 (1C), 190.9 (4C, br), 185.9 (1C), 182.1 (1C, br); δ 176.3 (C_α), 147.6 (*J*_{WC} = 60 Hz, C_β), 135.5 (*i*-C₆H₅), 131.3 (2C, *o*-C₆H₅), 128.8 (2C, *m*-C₆H₅), 128.3 (*p*-C₆H₅), 114.0 (C₅Me₅), 10.6 (C₅Me₅). Anal. Calcd for C₂₇H₂₀O₁₀Re₂W: C, 30.57; H, 1.90. Found: C, 30.41; H, 1.96.

Spectral data for **4b**: MS (FAB, ¹⁸⁴W, ¹⁸⁷Re) *m/z* 1026 (M⁺). IR C₆H₁₂ ν(CO): 2110 (s), 2052 (m), 2031 (vw), 2014 (vs), 2005 (vs), 1988 (w), 1976 (s), 1965 (w), 1808 (vw, br) cm⁻¹. ¹H NMR (300 MHz, CDCl₃, 294 K): δ 5.54 (s, 1H), 5.46 (s, 1H), 2.37 (s, 3H, Me), 2.01 (s, 15H, Cp*). ¹³C NMR (100.6 MHz, CDCl₃, 294 K): CO, δ 226.6 (*J*_{WC} = 42 Hz, 1C), 194.5 (1C), 191.9 (1C), 191.0 (4C, br), 186.1 (1C), 182.2 (1C, br); δ 175.6 (C_α), 148.8 (*J*_{WC} = 61 Hz, C_β), 138.8 (C_γ), 119.7 (CH₂), 114.1 (C₅Me₅), 25.3 (Me), 10.7 (C₅Me₅). Anal. Calcd for C₂₄H₂₀O₁₀Re₂W: C, 28.13; H, 1.97. Found: C, 28.08; H, 2.10.

Thermolysis of **4a.** A toluene solution (30 mL) of **4a** (26.6 mg, 0.026 mmol) was refluxed under nitrogen for 3 h, during which the color changed from orange to red. After removal of the solvent, the residue was dissolved in CH₂Cl₂ and then separated using thin-layer chromatography (dichloromethane:hexane = 1:2), giving 21.5 mg of **2a** (0.022 mmol, 83%).

Hydrogenation of **2a.** A toluene solution (60 mL) of **2a** (150 mg, 0.145 mmol) was heated at reflux under hydrogen (1 atm) for 1.5 h, during which the color changed from orange to red-brown. After the solution was allowed to reach room

(7) Wu, H.-L.; Lu, G.-L.; Chi, Y.; Farrugia, L. J.; Peng, S.-M.; Lee, G.-H. *Inorg. Chem.* **1996**, *35*, 6015.

(8) Peng, J.-J.; Peng, S.-M.; Lee, G.-H.; Chi, Y. *Organometallics* **1995**, *14*, 626.

(9) (a) Bruce, M. I.; Humphrey, M. G.; Matison, J. G.; Roy, S. K.; Swincer, A. G. *Aust. J. Chem.* **1984**, *37*, 1955. (b) Harris, G. W.; Boeyens, J. C. A.; Coville, N. J. *J. Chem. Soc., Dalton Trans.* **1985**, 2277.

temperature, the solvent was evaporated and the residue was taken in CH_2Cl_2 and separated by TLC (dichloromethane:hexane = 1:1), giving 31 mg of dark-red $\text{Cp}^*\text{WRe}_2(\mu\text{-O})(\mu\text{-H})_2\text{-}(\text{CCPh})(\text{CO})_6$ (**5a**, 0.032 mmol, 22%), 39 mg of orange $\text{Cp}^*\text{W}(\text{O})\text{Re}_2(\mu\text{-CHCHPh})(\text{CO})_8$ (**6a**, 0.038 mmol, 26%), and 22 mg of yellow $\text{Cp}^*\text{W}(\text{O})\text{Re}_2(\mu\text{-H})(\mu\text{-CHCH}_2\text{Ph})(\text{CO})_8$ (**7a**, 0.021 mmol, 14%). Crystals of **6a** and **7a** suitable for X-ray diffraction study were recrystallized at room temperature from a layered solution of chloroform–hexane and chloroform–methanol, respectively.

In an another experiment, a heptane solution (30 mL) of **2a** (25 mg, 0.024 mmol) was heated at reflux under hydrogen (1 atm) for 40 min. After removal of the heptane in vacuo, the residue was dissolved in a minimum amount of CH_2Cl_2 and passed through a short silica gel column to remove the trace amount of decomposition product. The ^1H NMR analysis indicated that the relative yields of complexes **2a**, **5a**, **6a**, and **7a** were 12%, 40%, 24%, and 5%, respectively.

Spectral data for **5a**: MS (FAB, ^{184}W , ^{187}Re) m/z 980 (M^+). IR (C_6H_{12}) $\nu(\text{CO})$: 2052 (vs), 2017 (vs), 1971 (vs), 1954 (vs), 1938 (m), 1932 (s) cm^{-1} . ^1H NMR (400 MHz, CDCl_3 , 294 K): δ 7.92 (d, 2H, $J_{\text{HH}} = 8$ Hz), 7.53 (t, 2H, $J_{\text{HH}} = 7.2$ Hz), 7.38 (t, 1H, $J_{\text{HH}} = 7.2$ Hz), 2.09 (s, 15H, C_5Me_5), -7.44 (s, 1H, $J_{\text{WH}} = 135$ Hz), -14.08 (s, 1H). ^{13}C NMR (100 MHz, CDCl_3 , 294 K): CO, δ 194.5 (br), 193.9, 189.9, 189.0 (br), 188.1, 184.2 (br); δ 156.6 (CCPh), 137.4, 132.4 (2C), 129.8, 128.9 (2C), 121.6 ($J_{\text{WC}} = 71$ Hz, CPh), 114.3 (C_5Me_5), 11.6 (C_5Me_5). Anal. Calcd for $\text{C}_{24}\text{H}_{22}\text{O}_7\text{Re}_2\text{W}_1\cdot\frac{1}{2}\text{CHCl}_3$: C, 28.34; H, 2.18. Found: C, 28.28; H, 2.25.

Spectral data for **6a**: MS (FAB, ^{184}W , ^{187}Re) m/z 1036 (M^+). IR (C_6H_{12}) $\nu(\text{CO})$: 2088 (m), 2043 (s), 2008 (vs), 1992 (vs), 1981 (s), 1961 (vw), 1942 (w), 1919 (s) cm^{-1} . ^1H NMR (400 MHz, CDCl_3 , 294 K): δ 7.42–7.21 (m, 5H, C_6H_5), 5.93 (d, 1H, $^3J_{\text{HH}} = 13.6$ Hz), 4.72 (d, 1H, $^3J_{\text{HH}} = 13.6$ Hz), 2.22 (s, 15H, C_5Me_5). ^{13}C NMR (100 MHz, CDCl_3 , 294 K): CO, δ 207.3, 205.4, 202.3, 196.3, 189.7, 189.1, 186.2, 183.5; δ 161.3 ($J_{\text{WC}} = 115$ Hz, CHCHPh), 142.9, 129.4 (2C), 127.9, 125.7 (2C), 112.2 (C_5Me_5), 76.8 (CHCHPh), 12.3 (C_5Me_5). Anal. Calcd for $\text{C}_{27}\text{H}_{24}\text{O}_9\text{Re}_2\text{W}_1\text{Cl}_2$: C, 28.96; H, 2.16. Found: C, 29.39; H, 2.18.

Spectral data for **7a**: MS (FAB, ^{184}W , ^{187}Re) m/z 1038 (M^+). IR (C_6H_{12}) $\nu(\text{CO})$: 2087 (s), 2041 (s), 2000 (vs), 1987 (vs), 1974 (w), 1963 (w), 1943 (w, br) cm^{-1} . ^1H NMR (300 MHz, CDCl_3 , 294 K): δ 7.42–7.30 (m, 5H, C_6H_5), 7.15 (dd, 1H, $^3J_{\text{HH}} = 9.8$ and 5.5 Hz), 4.65 (dd, 1H, $^2J_{\text{HH}} = 14$ Hz, $^3J_{\text{HH}} = 5.5$ Hz), 4.13 (d, 1H, $^2J_{\text{HH}} = 14$ Hz, $^3J_{\text{HH}} = 9.8$ Hz), 2.08 (s, 15H, C_5Me_5), -10.93 (s, 1H, $J_{\text{WH}} = 97.2$ Hz). ^{13}C NMR (75 MHz, CDCl_3 , 294 K): CO, δ 198.3, 193.9, 193.8, 193.1, 192.3, 191.2, 190.8, 190.1; δ 146.7, 141.6 ($J_{\text{WC}} = 104$ Hz, CHCH $_2$ Ph), 128.6 (2C), 128.5 (2C), 126.7, 114.0 (C_5Me_5), 61.7 (CHCH $_2$ Ph), 11.6 (C_5Me_5). Anal. Calcd for $\text{C}_{26}\text{H}_{24}\text{O}_9\text{Re}_2\text{W}_1$: C, 30.12; H, 2.33. Found: C, 29.96; H, 2.35.

Treatment of 5a with CO. A heptane solution (30 mL) of **5a** (13 mg, 0.013 mmol) was heated at reflux under CO (1 atm) for 2 min. During which the color changed from yellow to red-orange. The solvent was then evaporated, the residue was taken up in CH_2Cl_2 and separated by thin-layer chromatography (dichloromethane:hexane = 1:2), giving 2.3 mg of **2a** (0.0022 mmol, 17%) and 2.7 mg of **6a** (0.0026 mmol, 20%).

Hydrogenation of 6a. A toluene solution (25 mL) of **6a** (22 mg, 0.021 mmol) was heated under hydrogen (3 atm) in a pressure bottle at 85 $^\circ\text{C}$ for 1.5 h, during which the color changed from yellow-orange to red-orange. After the solution was cooled to room temperature, the solvent was evaporated and the residue was dissolved in a minimum amount of CH_2Cl_2 and separated by thin-layer chromatography (dichloromethane:hexane = 1:2), giving 2.3 mg of **6a** (0.0022 mmol, 10%) and 9.2 mg of yellow **7a** (0.0088 mmol, 42%) as the major products. The deuterium labeled compound **7a** with formula $\text{Cp}^*\text{W}(\text{O})\text{Re}_2(\mu\text{-D})(\mu\text{-CHCHDPh})(\text{CO})_8$ was prepared from the reaction with D_2 under similar conditions.

Thermolysis of 6a. A toluene solution (15 mL) of **6a** (9.5 mg, 0.009 mmol) was refluxed under a nitrogen atmosphere (1 atm) for 2 h. After removal of the solvent, the residue was

taken up in CH_2Cl_2 and separated by thin-layer chromatography (dichloromethane:hexane = 1:2), giving 0.3 mg of **2a** (0.004 mmol, 3%) and 3.1 mg of **5a** (0.004 mmol, 35%), in addition to 4.2 mg of unreacted **6a** (0.009 mmol, 44%).

Thermolysis of 7a. A toluene solution (30 mL) of **7a** (36 mg, 0.034 mmol) was refluxed under nitrogen for 2 h, during which the color changed from yellow to orange. After removal of the solvent, the residue was taken up in CH_2Cl_2 and separated by thin-layer chromatography (dichloromethane:hexane = 1:2), giving 4.1 mg of **5a** (0.004 mmol, 12%), 19 mg of **6a** (0.019 mmol, 55%), and 9.2 mg of unreacted **7a** (0.009 mmol, 25%).

Hydrogenation of 2b. A toluene solution (50 mL) of **2b** (50.4 mg, 0.051 mmol) was heated at reflux under hydrogen (1 atm) for 30 min, during which the color changed from orange to red-brown. After removal of the solvent, the residue was taken up in CH_2Cl_2 and separated by thin-layer chromatography (dichloromethane:hexane = 1:2), giving 2 mg of yellow $\text{Cp}^*\text{W}(\text{O})\text{Re}_2(\mu\text{-H})[\mu\text{-CHCH}_2\text{C}(\text{Me})=\text{CH}_2](\text{CO})_8$ (**7b**, 0.002 mmol, 4%), 16 mg of brown $\text{Cp}^*\text{WRe}_2(\mu\text{-O})(\mu\text{-H})_2[\mu\text{-CCC}(\text{Me})=\text{CH}_2](\text{CO})_6$ (**5b**, 0.016 mmol, 32%), 7.5 mg of orange $\text{Cp}^*\text{W}(\text{O})\text{Re}_2[\mu\text{-CHCHC}(\text{Me})=\text{CH}_2](\text{CO})_8$ (**6b**, 0.008 mmol, 15%), and 8.7 mg of red-brown $\text{Cp}^*\text{WRe}_2(\mu\text{-O})[\mu\text{-CHCC}(\text{Me})_2](\text{CO})_7$ (**8**, 0.009 mmol, 18%), in the order of their elution. Crystals of **8** suitable for X-ray diffraction study were obtained from a layered solution of chloroform–heptane at room temperature.

Spectral data for **5b**: MS (FAB, ^{184}W , ^{187}Re) m/z 944 (M^+). IR (C_6H_{12}) $\nu(\text{CO})$: 2052 (s), 2017 (vs), 1970 (s, br), 1954 (s, br), 1938 (m, br), 1932 (m, br) cm^{-1} . ^1H NMR (300 MHz, CDCl_3 , 294 K): δ 5.72 (1H, CH_2), 5.65 (1H, CH_2), 2.41 (s, 3H, Me), 2.11 (s, 15H, Cp^*), -7.59 (s, $J_{\text{WH}} = 135.6$ Hz, 1H), -14.18 (s, 1H).

Spectral data for **6b**: MS (FAB, ^{184}W , ^{187}Re) m/z 1000 (M^+). IR (C_6H_{12}) $\nu(\text{CO})$: 2088 (m), 2043 (s), 2007 (vs), 1989 (vs), 1980 (s), 1961 (vw, br), 1942 (w, br), 1918 (s) cm^{-1} . ^1H NMR (300 MHz, CDCl_3 , 294 K): δ 5.41 (s, 1H), 5.35 (s, 1H), 5.22 (d, $J_{\text{HH}} = 13.7$ Hz, 1H, C_αH), 4.60 (d, $J_{\text{HH}} = 13.7$ Hz, 1H, C_βH), 2.18 (s, 15H, Cp^*), 1.61 (s, 3H, Me). ^{13}C NMR (75.5 MHz, CDCl_3 , 294 K): CO, δ 207.4, 205.5, 202.3, 196.4, 189.9, 188.9, 186.5, 183.8; δ 160.2 ($J_{\text{WC}} = 114$ Hz, C_αH), 145.3 (C_γ), 118.1 (C_5Me_5), 112.0 (C_βH), 84.4 (CH_2), 16.4 (Me), 12.2 (C_5Me_5). Anal. Calcd for $\text{C}_{23}\text{H}_{22}\text{O}_9\text{Re}_2\text{W}$: C, 27.66; H, 2.22. Found: C, 27.52; H, 2.28.

Spectral data for **7b**: MS (FAB, ^{184}W , ^{187}Re) m/z 1002 (M^+). IR (C_6H_{12}) $\nu(\text{CO})$: 2087 (s), 2041 (vs), 2001 (vs), 1987 (vs, br), 1962 (w), 1942 (s, br) cm^{-1} . ^1H NMR (400 MHz, CDCl_3 , 294 K): δ 7.13 (dd, $J_{\text{HH}} = 11.2$ and 3.2 Hz, 1H), 4.97 (s, 1H), 4.91 (s, 1H), 4.05 (d, $J_{\text{HH}} = 14.8$ and 3.2 Hz, 1H), 3.57 (dd, $J_{\text{HH}} = 14.8$ and 11.2 Hz, 1H), 2.07 (s, 15H, Cp^*), 2.00 (s, 3H, Me), -10.84 (s, $J_{\text{WH}} = 97.6$ Hz, 1H). ^{13}C NMR (75.5 MHz, CDCl_3 , 294 K): CO, δ 199.3 (br), 194.0, 193.8 (br), 193.0, 192.3, 191.2 (br), 190.7, 190.1; δ 149.1 (C_γ), 137.0 ($J_{\text{WC}} = 104$ Hz, C_αH), 113.8 (C_5Me_5), 112.4 (CH_2), 63.7 (C_β), 21.8 (Me), 11.6 (C_5Me_5). Anal. Calcd for $\text{C}_{23}\text{H}_{24}\text{O}_9\text{Re}_2\text{W}$: C, 27.61; H, 2.42. Found: C, 27.43; H, 2.41.

Spectral data for **8**: MS (FAB, ^{184}W , ^{187}Re) m/z 972 (M^+). IR (C_6H_{12}) $\nu(\text{CO})$: 2046 (s), 2010 (vs), 1972 (s), 1963 (w), 1936 (s), 1919 (w), 1777 (vw, br) cm^{-1} . ^1H NMR (300 MHz, CDCl_3 , 294 K): δ 9.23 (s, 1H, C_αH), 2.22 (s, 3H, Me), 2.09 (s, 15H, Cp^*), 1.79 (s, 3H, Me). ^{13}C NMR (100.6 MHz, CDCl_3 , 294 K): CO, δ 251.9 ($J_{\text{WC}} = 133$ Hz, 1C), 200.0 (1C), 197.4 (4C), 188.9 (1C); δ 165.0 (C_β), 136.0 ($J_{\text{WC}} = 97$ Hz, C_αH), 112.7 (C_5Me_5), 66.0 (C_γ), 27.4 (2Me), 10.1 (C_5Me_5). Anal. Calcd for $\text{C}_{22}\text{H}_{22}\text{O}_8\text{Re}_2\text{W}$: C, 27.22; H, 2.28. Found: C, 27.11; H, 2.26.

Hydrogenation of 6b. To a 300 mL glass pressure bottle, toluene (30 mL) and **6b** (25.8 mg, 0.026 mmol) were added. The bottle was charged with 3 atm of hydrogen and placed into a preheated oil bath maintained at 90 $^\circ\text{C}$ for 2 h. After removal of the solvent, the residue was taken up in CH_2Cl_2 and separated by thin-layer chromatography (dichloromethane:hexane = 1:2), producing 4 mg of yellow **7b** (0.004 mmol, 15%) together with 12.8 mg of **6b**.

Thermolysis of 7b. A toluene solution (30 mL) of **7b** (10.8 mg, 0.011 mmol) was heated at reflux under nitrogen for 2 h.

Table 1. Experimental Data for the X-ray Diffraction Studies of Complexes 4a, 6a, 7a, and 8^a

	4a	6a	7a	8
formula	C ₂₇ H ₂₀ O ₁₀ Re ₂ W	C ₂₆ H ₂₂ O ₉ Re ₂ W·1/2CH ₂ Cl ₂	C ₂₆ H ₂₄ O ₉ Re ₂ W	C ₂₂ H ₂₂ O ₈ Re ₂ W
mw	1060.71	1077.18	1036.73	970.68
cryst syst	trigonal	monoclinic	orthorhombic	monoclinic
space group	R $\bar{3}$	C2/c	P2 ₁ 2 ₁ 2 ₁	P2 ₁ /n
a (Å)	41.77(1)	16.847(5)	11.743(4)	10.542(2)
b (Å)		16.303(5)	12.922(4)	14.713(3)
c (Å)	9.386(5)	23.044(4)	18.794(4)	16.138(4)
β (deg)		111.26(2)		98.62(2)
volume (Å ³)	14 179(8)	5898(3)	2852(1)	2475(1)
Z	18	8	4	4
D _c (g/cm ³)	2.236	2.426	2.415	2.605
F(000)	8748	3960	1904	1768
2 θ (max)	50°	45°	50°	50°
h,k,l ranges	−41 to 42, 0–49, 0–11	−18 to 16, 0–17, 0–24	−0 to 13, 0–15, 0–22	−12 to 12, 0–17, 0–19
cryst size (mm)	0.20 × 0.20 × 0.50	0.25 × 0.35 × 0.45	0.20 × 0.25 × 0.40	0.13 × 0.25 × 0.35
μ (Mo K α) (cm ^{−1})	115.40	123.18	127.39	146.76
transmission: max, min	1.00, 0.47	1.00, 0.67	1.00, 0.38	1.00, 0.41
no. of unique data	5545	3859	2826	4344
no. of data with $I > 2\sigma(I)$	3695	3250	2491	3474
no. of atoms, params	60, 362	63, 358	61, 344	55, 299
weight modifier (g)	0.00001	unit weight	unit weight	unit weight
maximum Δ/σ ratio	0.056	0.010	0.045	0.006
R_F , R_w	0.040; 0.047	0.025; 0.022	0.029; 0.023	0.036; 0.031
GOF	2.90	1.87	1.66	2.47
diff map, max/min (e/Å ³)	1.49/−1.13	2.42/−0.72	1.30/−0.80	1.30/−1.87

^a Features common to all determinations: Nonius CAD-4 diffractometer, $\lambda(\text{Mo K}\alpha) = 0.7107 \text{ \AA}$; minimize function: $\sum(w|F_o - F_c|^2)$, weighting scheme: $w^{-1} = \sigma^2(F_o) + |g|F_o^2$; GOF = $[\sum w|F_o - F_c|^2 / (N_o - N_v)]^{1/2}$ (N_o = number of observations; N_v = number of variables).

After removal of the solvent in vacuo, the oily residue was dissolved in dichloromethane and passed through a short silica gel column to remove trace amount of decomposition product. The ¹H NMR analysis indicated that the relative yields of **6b**, **7b**, and **8** were 5%, 13%, and 15%, respectively.

Thermolysis of 6b. A toluene solution (30 mL) of **6b** (23.8 mg, 0.024 mmol) was heated at reflux under nitrogen for 2 h. After removal of the solvent, the residue was taken up in CH₂Cl₂ and separated by thin-layer chromatography (dichloromethane:hexane = 1:2), giving 5.5 mg of red-brown **8** (0.0057 mmol, 24%) and 4.3 mg of unreacted **6b**.

X-ray Crystallography. The X-ray diffraction measurements were carried out on a Nonius CAD-4 diffractometer at room temperature. Lattice parameters were determined from 25 randomly selected high-angle reflections. Three standard reflections were monitored every 3600 s. No significant change in intensities, due to crystal decay, was observed over the course of all data collection. Intensities of the diffraction signals were corrected for Lorentz, polarization, and absorption effects (ψ scans). The structure was solved by using the NRCC-SDP-VAX package. All the non-hydrogen atoms had anisotropic temperature factors, while the hydrogen atoms of the organic substituents were placed at the calculated positions with $U_H = U_C + 0.1$. The experimental data of the X-ray diffraction studies of **2b** and **5a** have been reported in a previous communication; therefore, these data were not duplicated in this article.⁶ The refinement parameters of complexes **4a**, **6a**, **7a** and **8** are given in Table 1, while their selected bond distances and angles are presented in Tables 2–5, respectively.

Results

Syntheses and Characterization of Oxo–Acetylide Complexes 2 and 4. Treatment of Cp*WRe₂(CCR)(CO)₉ (**1a**, R = Ph; **1b**, R = C(Me)=CH₂) with oxygen or nitrous oxide gave the oxo compound Cp*W(O)(Re₂CCR)(CO)₈ (**2a**, R = Ph; **2b**, R = C(Me)=CH₂) in 48–64% yields, based on the starting materials consumed. These compounds have been characterized by a combination of microanalysis, solution IR studies ¹H and ¹³C NMR studies, and the X-ray diffraction study on **2b**.

Table 2. Selected Bond Distances (Å) and Bond Angles (deg) of 4a (Esd in Parentheses)

W–Re(1)	2.906(1)	Re(1)–Re(2)	3.010(1)
W–O(10)	1.71(1)	W–C(10)	2.12(2)
W–C(11)	2.12(2)	Re(1)–C(10)	2.01(1)
C(10)–C(11)	1.27(2)	W–C(1)	2.41(2)
Re(1)–C(1)	2.00(2)	Re(1)–C(2)	2.05(2)
Re(1)–C(3)	2.00(2)	Re(1)–C(4)	2.02(2)
Re(2)–C(5)	2.01(2)	Re(2)–C(6)	2.02(2)
Re(2)–C(7)	1.93(2)	Re(2)–C(8)	2.00(2)
Re(2)–C(9)	2.02(2)		
W–Re(1)–Re(2)	135.64(4)	Re(2)–Re(1)–C(1)	167.5(5)
Re(1)–Re(2)–C(7)	178.1(6)	Re(2)–Re(1)–C(10)	89.0(5)
Re(1)–C(10)–C(11)	162(1)	Re(1)–C(1)–O(1)	152(2)
Re–C–O (terminal)	177(2)		

Table 3. Selected Bond Distances (Å) and Bond Angles (deg) of 6a (Esd in Parentheses)

W–Re(1)	3.061(1)	W–Re(2)	2.7624(8)
Re(1)–Re(2)	3.0943(8)	W–O(9)	1.701(6)
W–C(9)	2.057(9)	Re(1)–C(9)	2.313(8)
C(9)–C(10)	1.39(1)	Re(1)–C(10)	2.394(8)
Re(1)–C(1)	1.95(1)	Re(1)–C(2)	1.98(1)
Re(1)–C(3)	1.941(9)	Re(1)–C(4)	1.98(1)
Re(2)–C(5)	1.96(1)	Re(2)–C(6)	1.912(9)
Re(2)–C(7)	1.97(1)	Re(2)–C(8)	1.88(1)
W–Re(1)–Re(2)	53.33(2)	W–Re(2)–Re(1)	62.72(2)
Re(1)–W–Re(2)	63.95(2)	W–C(9)–C(10)	129.0(7)
C(9)–C(10)–C(11)	124.4(8)	Re–C–O (terminal)	177(1)

As indicated in Figure 1, the structure of **2b** consists of an L-shaped core arrangement with eight terminal CO ligands, four on each Re atom. The acetylide ligand adopts a novel $\mu_3, \eta^1, \eta^1, \eta^2$ -mode, which is in sharp contrast to the typical edge-bridging μ, η^1, η^2 -mode or the face-capping $\mu_3, \eta^1, \eta^2, \eta^2$ -mode observed in other cluster compounds.¹⁰ The α -carbon C(9) is linked to all three metal atoms with distances in the range 2.160(7)–2.215(9) Å, but the β -carbon C(10) is bonded only to the W atom, with substantial carbenic bonding character,

(10) (a) Cherkas, A. A.; Taylor, N. J.; Carty, A. J. *J. Chem. Soc., Chem. Commun.* **1990**, 385. (b) Deeming, A. J.; Donovan-Mtunzi, S.; Hardcastle, K. *J. Chem. Soc., Dalton Trans.* **1986**, 543. (c) Boyar, E.; Deeming, A. J.; Felix, M. S. B.; Kabir, S. E.; Adatia, T.; Bhusate, R.; McPartlin, M.; Powell, H. R. *J. Chem. Soc. Dalton Trans.* **1989**, 5.

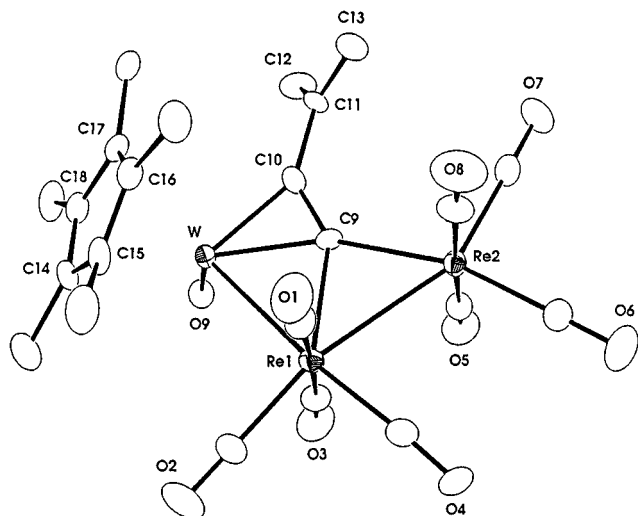


Figure 1. Molecular structure of $\text{Cp}^*\text{W}(\text{O})\text{Re}_2[\text{CCC}(\text{Me})=\text{CH}_2](\text{CO})_8$ (**2b**) and selected bond lengths (Å) and angles (deg): $\text{W}-\text{Re}(1) = 2.7544(8)$, $\text{Re}(1)-\text{Re}(2) = 2.9167(9)$, $\text{W}-\text{O}(9) = 1.699(6)$, $\text{W}-\text{C}(9) = 2.182(9)$, $\text{W}-\text{C}(10) = 2.012(9)$, $\text{Re}(1)-\text{C}(9) = 2.160(7)$, $\text{Re}(2)-\text{C}(9) = 2.215(9)$, $\text{C}(9)-\text{C}(10) = 1.31(1)$, $\text{W}-\text{C}(10)-\text{C}(9) = 79.0(6)$, $\text{Re}(2)-\text{C}(9)-\text{C}(10) = 132.8(7)$.

Table 4. Selected Bond Distances (Å) and Bond Angles (deg) of 7a (Esd in Parentheses)

$\text{W}-\text{Re}(1)$	2.850(1)	$\text{W}-\text{Re}(2)$	3.045(1)
$\text{Re}(1)-\text{Re}(2)$	2.983(1)	$\text{W}-\text{O}(9)$	1.686(9)
$\text{W}-\text{C}(9)$	2.05(2)	$\text{Re}(1)-\text{C}(9)$	2.20(1)
$\text{Re}(1)-\text{C}(1)$	1.92(2)	$\text{Re}(1)-\text{C}(2)$	1.99(1)
$\text{Re}(1)-\text{C}(3)$	1.98(1)	$\text{Re}(1)-\text{C}(4)$	1.93(1)
$\text{Re}(2)-\text{C}(5)$	1.96(2)	$\text{Re}(2)-\text{C}(6)$	1.87(2)
$\text{Re}(2)-\text{C}(7)$	1.93(2)	$\text{Re}(2)-\text{C}(8)$	1.76(2)
$\text{W}-\text{Re}(1)-\text{Re}(2)$	62.88(2)	$\text{W}-\text{Re}(2)-\text{Re}(1)$	56.43(2)
$\text{Re}(1)-\text{W}-\text{Re}(2)$	60.69(3)	$\text{W}-\text{C}(9)-\text{Re}(1)$	84.3(5)
$\text{W}-\text{Re}(2)-\text{C}(5)$	78.8(4)	$\text{W}-\text{Re}(2)-\text{C}(7)$	102.5(4)
$\text{W}-\text{Re}(2)-\text{C}(8)$	110.4(6)	$\text{Re}-\text{C}-\text{O}$ (terminal)	175(1)

Table 5. Selected Bond Distances (Å) and Bond Angles (deg) of 8 (Esd in Parentheses)

$\text{W}-\text{Re}(1)$	2.8827(9)	$\text{W}-\text{Re}(2)$	2.7884(9)
$\text{Re}(1)-\text{Re}(2)$	2.919(1)	$\text{W}-\text{O}(8)$	1.800(9)
$\text{Re}(2)-\text{O}(8)$	2.141(8)	$\text{W}-\text{C}(8)$	2.09(1)
$\text{Re}(1)-\text{C}(8)$	2.26(1)	$\text{Re}(1)-\text{C}(9)$	2.17(1)
$\text{Re}(2)-\text{C}(9)$	2.26(1)	$\text{Re}(2)-\text{C}(10)$	2.49(1)
$\text{C}(8)-\text{C}(9)$	1.48(2)	$\text{C}(9)-\text{C}(10)$	1.34(2)
$\text{W}-\text{C}(1)$	1.98(1)	$\text{Re}(1)-\text{C}(1)$	2.49(1)
$\text{Re}(1)-\text{C}(2)$	1.97(2)	$\text{Re}(1)-\text{C}(3)$	1.92(2)
$\text{Re}(1)-\text{C}(4)$	2.00(1)	$\text{Re}(2)-\text{C}(5)$	1.95(1)
$\text{Re}(2)-\text{C}(6)$	1.95(1)	$\text{Re}(2)-\text{C}(7)$	1.98(1)
$\text{W}-\text{Re}(1)-\text{Re}(2)$	57.45(2)	$\text{W}-\text{Re}(2)-\text{Re}(1)$	60.63(2)
$\text{Re}(1)-\text{W}-\text{Re}(2)$	61.93(2)	$\text{W}-\text{O}(8)-\text{Re}(2)$	89.6(4)
$\text{W}-\text{C}(1)-\text{O}(1)$	159(1)	$\text{C}(8)-\text{C}(9)-\text{C}(10)$	139(1)
$\text{Re}-\text{C}-\text{O}$ (terminal)	177(1)		

$\text{W}-\text{C}(10) = 2.012(9)$ Å. In accordance with this bonding mode, the α - and β -resonances of the acetylide of **2a** and **2b** appeared at δ 184.6 and 211.4 ($J_{\text{WC}} = 77$ Hz) and at δ 181.9 and 212.8 ($J_{\text{WC}} = 72$ Hz) in the ^{13}C NMR spectrum. The downfield shift of the β -carbon atoms with respect to the α -carbons is obviously due to the $\text{W}=\text{C}$ carbenic character and is confirmed by the observation of large J_{WC} coupling constants.

In addition, the oxo ligand adopts a terminal mode, and the resulting $\text{W}-\text{O}$ vector is perpendicular to the plane defined by the metal atoms and the acetylide ligand. This ligand arrangement is probably due to the availability of the d-orbitals in forming both the σ -bonding and π -interaction to the oxygen atom. Although the

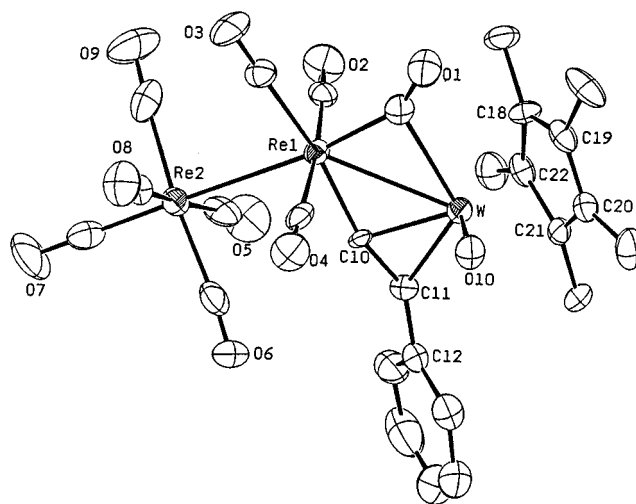
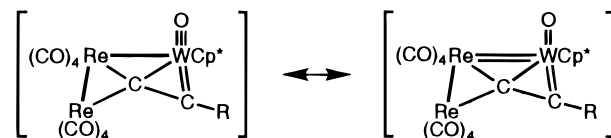


Figure 2. Molecular structure of $\text{Cp}^*\text{W}(\text{O})\text{Re}_2(\text{CCPh})(\text{CO})_9$ (**4a**), showing the atomic labeling scheme and the thermal ellipsoids at 30% probability level.

$\text{W}-\text{O}(9)$ distance (1.699(6) Å) is similar to that observed in W_2Fe and WCo oxo compounds¹¹ and in the W_2Ru_4 cluster with the $\text{Cp}^*\text{W}(\text{O})$ fragment,¹² it cannot be utilized for identifying the nature of bonding, as the actual bonding mode (double bond vs triple bond) is determined by its donor capability (two-electron vs four-electron on a covalent model) and because the respective $\text{W}-\text{O}$ interactions show little variation in bond distances.¹³ However, we propose that the $\text{W}-\text{O}$ interaction presents a $\text{W}=\text{O}$ triple bond on the basis of electron counting. In this way, if the oxo ligand is regarded as a four-electron donor in the covalent model, the number of valence electrons satisfies the prediction of 50 electrons for a trinuclear compound with two metal-metal bonds.

Conversely, the relatively short $\text{W}-\text{Re}(1)$ distance (2.7544(8) Å) observed in **2b** falls between that of the $\text{W}=\text{Re}$ double bond (2.672 Å) and $\text{W}-\text{Re}$ single bond (2.898 Å) in the WRe_2 cluster $\text{Cp}^*\text{WRe}_2(\mu\text{-H})[\text{CHCHC}(\text{Me})\text{CH}](\text{CO})_7$.¹⁴ This suggests that this $\text{W}-\text{Re}(1)$ bonding may possess some $\text{W}=\text{Re}$ double-bond bonding character. This leads us to believe that the actual bonding interaction of this cluster contains some contribution from the second structure, shown. The latter



possesses $\text{W}=\text{Re}$ and $\text{W}=\text{O}$ double bonds and is complementary to the originally proposed structure involving a $\text{W}-\text{Re}$ single bond and a $\text{W}=\text{O}$ triple bond.

Complexes **2a** and **2b** were transformed into two new compounds $\text{Cp}^*\text{W}(\text{O})\text{Re}_2(\text{CCPh})(\text{CO})_9$ (**4a**, $\text{R} = \text{Ph}$; **4b**, $\text{R} = \text{C}(\text{Me})=\text{CH}_2$) in nearly quantitative yields, when heated to 90 °C under a CO atmosphere in toluene. An ORTEP drawing of derivative **4a** is shown in Figure 2,

(11) (a) Busetto, L.; Jeffery, J. C.; Mills, R. M.; Stone, F. G. A.; Went, M. J.; Woodward, P. *J. Chem. Soc., Dalton Trans.* **1983**, 101. (b) El Amin, A. E.; Jeffery, J. C.; Walters, T. M. *J. Chem. Soc., Chem. Commun.* **1990**, 170.

(12) Su, C.-J.; Su, P.-C.; Chi, Y.; Peng, S.-M.; Lee, G.-H. *J. Am. Chem. Soc.* **1996**, *118*, 3289.

(13) Mayer, J. M. *Inorg. Chem.* **1988**, *27*, 3899.

(14) Cheng, P.-S.; Chi, Y.; Peng, S.-M.; Lee, G.-H. *Organometallics* **1993**, *12*, 250.

and selected distances and angles are given in Table 1. The molecule was found to consist of an open triangular geometry with five terminal CO ligands attached to the Re(2) atom and three terminal and one *semi*-bridging CO ligand to the Re(1) atom. The equatorial CO ligands on Re atoms adopt the staggered conformation, as expected on steric grounds. The Re(1)–Re(2) distance of 3.010(1) Å is similar to that of Re₂(CO)₁₀ (3.041(1) Å)¹⁵ and the isonitrile compounds Re₂(CO)_xL_{10-x}, *x* = 1–3 (3.048–3.081 Å).¹⁶ The W–Re(1)–Re(2) angle is 135.64(4)°, which is more obtuse than that observed in its precursor **2b** (99.88(2)°) but is comparable to that reported in the open trinuclear clusters Os₃(CO)₁₁(μ-CNCF₃)₂ (140.39(4)°) and Os₃(μ-CNCF₃)₂(CO)₁₀(NCMe) (137.06(2)°), which contain at least one bridging isonitrile ligand on the Os–Os bond.¹⁷

The acetylide ligand in **4a** is associated with the Re–W bond. The C(10)–C(11) distance (1.27(2) Å) is slightly longer than those of the terminal acetylide ligands (1.19–1.21 Å)¹⁸ and is also comparable with that of the dinuclear oxo-acetylide complex Cp*Re(CO)(PMe₂Ph)(μ-C₂Ph)W(O)Cp (1.30(2) Å),¹⁹ indicating the existence of a weakened donor interaction from the acetylide ligand to the W atom. On the basis of this structural data and the elongated W–C(10) and W–C(11) distances observed, the acetylide is considered to behave as a three-electron donor, forming σ-bond to the central Re(1) atom and π-interaction to the W atom, respectively. In accordance, the ¹³C NMR signals of the acetylide α- and β-carbon atoms occur at δ 175.6 and 176.3 and at δ 147.6 and 148.8 with coupling constant *J*_{WC} = 60–61 Hz for complexes **4a** and **4b**, respectively. These high-field shifts with respect to those observed in **2** are consistent with the reduction of electron donation to the W atom via an interaction incorporating one set of π-orbitals.²⁰

Reaction of the Oxo-Acetylide Complex 2a with Hydrogen. Three new products were obtained from the hydrogenation of **2a** in heptane solution (1 atm, 90 °C, 40 min). These compounds were identified as Cp*WRe₂(μ-O)(μ-H)₂(CCPh)(CO)₆ (**5a**, dark-red, 50%), Cp*W(O)Re₂(μ-CHCHPh)(CO)₈ (**6a**, orange, 28%), and Cp*W(O)Re₂(μ-H)(μ-CHCH₂Ph)(CO)₈ (**7a**, yellow, 5%) and were characterized by spectroscopic methods and X-ray diffraction studies.

For complex **5a**, the ¹H NMR spectrum exhibits two signals at δ –7.44 (*J*_{WH} = 135 Hz) and –14.08 in addition to the Cp* and the phenyl signals, indicating the presence of two bridging hydride ligands. The acetylide signals appear at δ 156.6 and 121.6 (*J*_{WC} = 71 Hz) in the ¹³C NMR spectrum, which fall in the range expected for the acetylides with μ₃-η²-mode.²¹ As can

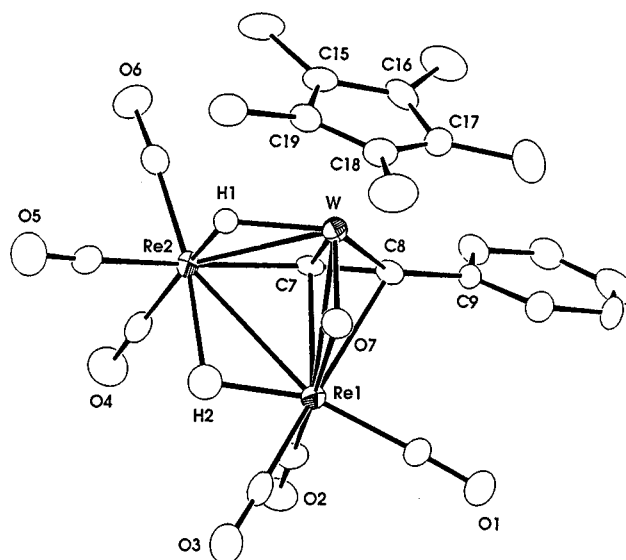


Figure 3. Molecular structure of Cp*WRe₂(μ-O)(μ-H)₂(CCPh)(CO)₆ (**5a**) and selected bond lengths (Å) and angles (deg): Re(1)–Re(2) = 3.0412(5), Re(1)–W = 2.8652(6), Re(2)–W = 2.9918(6), W–O(7) = 1.765(6), Re(1)–O(7) = 2.286(5), W–C(7) = 2.189(8), Re(1)–C(7) = 2.370(8), Re(2)–C(7) = 2.028(7), W–C(8) = 2.118(8), Re(1)–C(8) = 2.496(8), C(7)–C(8) = 1.34(1), W–H(1) = 1.78(6), Re(2)–H(1) = 1.86(6), Re(1)–H(2) = 1.78(7), Re(2)–H(2) = 2.03(8), W–O(7)–Re(1) = 89.1(2), Re(2)–C(7)–C(8) = 157.2(7), C(7)–C(8)–C(9) = 138.7(8).

be seen from Figure 3, the X-ray diffraction analysis reveals the triangular WRe₂ core geometry. The hydride ligands, which are unambiguously located on the electron density map, span the W–Re(2) and the Re(1)–Re(2) edge. Each Re atom is coordinated by three terminal CO ligands, and the acetylide is perpendicular to the W–Re(1) edge supporting the bridging oxo ligand. The oxo ligand has changed to an asymmetric W=O→Re bridging mode with distances W–O(7) = 1.765(6) Å and Re(1)–O(7) = 2.286(5) Å. These distances are similar to those in the WRu₄ cluster Cp*W(O)₂Ru₄(μ₄-PPh)(CCPh)(CO)₁₀²² and the trinuclear cluster Cp₂W₂Re(μ-Br)(μ-O)(μ-CTol)₂(CO)₃²³ and are also related to the W=O→Os mode of cluster compounds having the WOs₃(μ-O) core arrangement.²⁴

Compound **6a** is a trinuclear oxo-alkenyl complex with the same number of CO ligands. As depicted in Figure 4, the cluster core contains one Cp*W(O) fragment and two Re(CO)₄ units, with the alkenyl ligand μ-CH=CHPh bridging the longer W–Re(1) bond. Both Re atoms appear to adopt a pseudo-octahedral arrangement. The *trans*-alkenyl ligand, which is formally generated by the addition of H₂ across the acetylide, adopts the typical σ + π bonding mode. Consistent with this assignment were the ¹H NMR data of two doublets at δ 5.93 and 4.72 with coupling constant ³*J*_{HH} = 13.6 Hz and the distinctive signals at δ 161.3 (*J*_{WC} = 115 Hz) and 76.8 in its ¹³C NMR spectrum.

The alkylidene complex **7a** is the third product generated from this reaction. It can be obtained independently in high yield from hydrogenation of the

(15) Churchill, M. R.; Amoh, K. N.; Wasserman, H. J. *Inorg. Chem.* **1981**, *20*, 1609.

(16) Harris, G. W.; Boeyens, J. C. A.; Coville, N. J. *Organometallics* **1985**, *4*, 914.

(17) (a) Adams, R. D.; Chi, Y.; DesMarteau, D. D.; Lentz, D.; Marshall, R. *J. Am. Chem. Soc.* **1992**, *114*, 1919. (b) Adams, R. D.; Chi, Y.; DesMarteau, D. D.; Lentz, D.; Marshall, R.; Scherrmann, A. *J. Am. Chem. Soc.* **1992**, *114*, 10822.

(18) Manna, J.; John, K. D.; Hopkins, M. D. *Adv. Organomet. Chem.* **1995**, *38*, 79.

(19) Lai, N.-S.; Tu, W.-C.; Chi, Y.; Peng, S.-M.; Lee, G.-H. *Organometallics* **1994**, *13*, 4652.

(20) (a) Templeton, J. L.; Ward, B. C. *J. Am. Chem. Soc.* **1980**, *102*, 3288. (b) Templeton, J. L. *Adv. Organomet. Chem.* **1989**, *29*, 1.

(21) (a) Hwang, D.-K.; Chi, Y.; Peng, S.-M.; Lee, G.-H. *Organometallics* **1990**, *9*, 2709. (b) Carty, A. J.; Cherkas, A. A.; Randall, L. H. *Polyhedron* **1988**, *7*, 1045. (c) Chi, Y.; Su, P.-C.; Peng, S.-M.; Lee, G.-H. *Organometallics* **1995**, *14*, 5483.

(22) Blenkiron, P.; Carty, A. J.; Peng, S.-M.; Lee, G.-H.; Su, C.-J.; Shiu, C.-W.; Chi, Y. *Organometallics* **1997**, *16*, 519.

(23) Carriedo, G. A.; Jeffery, J. C.; Stone, F. G. A. *J. Chem. Soc., Dalton Trans.* **1984**, 1597.

(24) (a) Chi, Y.; Shapley, J. R.; Ziller, J. W.; Churchill, M. R. *Organometallics* **1987**, *6*, 301. (b) Gong, J.-H.; Chen, C.-C.; Chi, Y.; Wang, S.-L.; Liao, F.-L. *J. Chem. Soc., Dalton Trans.* **1993**, 1829.

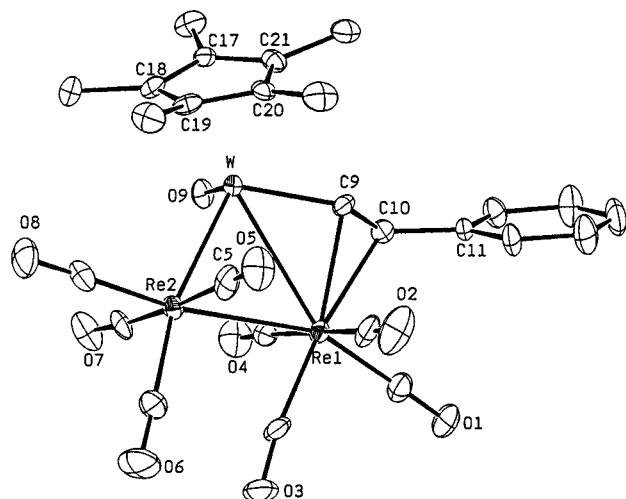


Figure 4. Molecular structure of $\text{Cp}^*\text{W}(\text{O})\text{Re}_2(\text{CHCHPh})(\text{CO})_8$ (**6a**), showing the atomic labeling scheme and the thermal ellipsoids at 30% probability level.

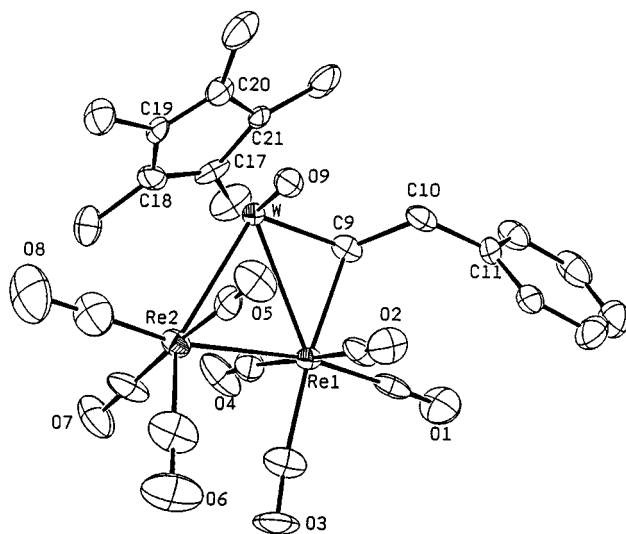


Figure 5. Molecular structure of $\text{Cp}^*\text{W}(\text{O})\text{Re}_2(\mu\text{-H})(\text{CHCH}_2\text{Ph})(\text{CO})_8$ (**7a**), showing the atomic labeling scheme and the thermal ellipsoids at 30% probability level.

alkenyl complex **6a** in toluene. The key spectral data comprises the ^{13}C NMR signals at δ 141.6 ($J_{\text{WC}} = 104$ Hz) and 61.7 due to the α -carbon of the alkylidene and the adjacent methylene group. The ^1H NMR spectrum agrees with this assignment, exhibiting three signals at δ 7.15, 4.65, and 4.13 with an ABX splitting pattern and a hydride signal at δ -10.93 ($J_{\text{WH}} = 97.2$ Hz). The ORTEP diagram depicted in Figure 5 exhibits the expected triangular WRe_2 skeletal arrangement with the alkylidene ligand, $\mu\text{-CHCH}_2\text{Ph}$, residing on the $\text{W-Re}(1)$ bond (2.950(1) Å). The hydride ligand, which is not located by difference Fourier synthesis, spans the second W-Re bond because of its longer bond distance (3.045(1) Å). The enlarged $\text{W-Re}(2)\text{-C}(7)\text{O}$ angle (102.5(4)°), which deviates substantially from the 90° angle of the octahedral environment, further confirms the assignment of hydride. Finally, the α -hydrogen of the alkylidene ligand is tilting away from the W=O fragment. This orientation reflects the absolute configuration of the alkenyl ligand in its precursor **6a**.

Reaction of the Oxo-Vinylacetylide Complex 2b with Hydrogen. Treatment of the vinylacetylide complex **1b** with hydrogen in refluxing toluene (1 atm, 30 min) afforded four products. These compounds were

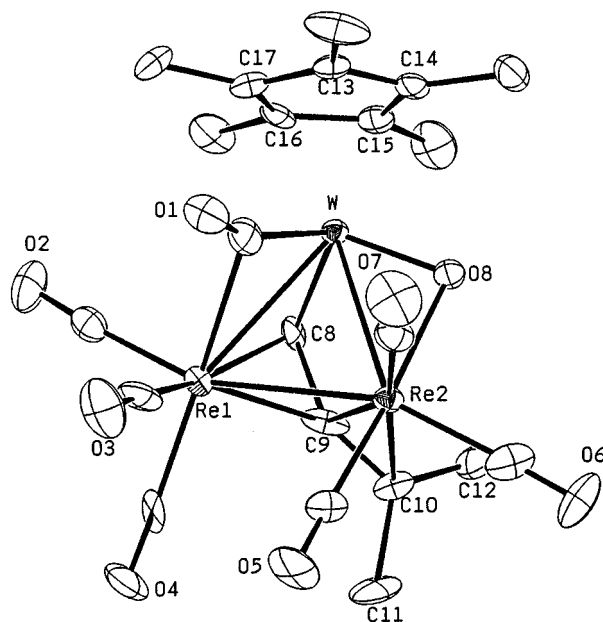


Figure 6. Molecular structure of $\text{Cp}^*\text{WRe}_2(\mu\text{-O})(\text{CHCMe}_2)(\text{CO})_7$ (**8**), showing the atomic labeling scheme and the thermal ellipsoids at 30% probability level.

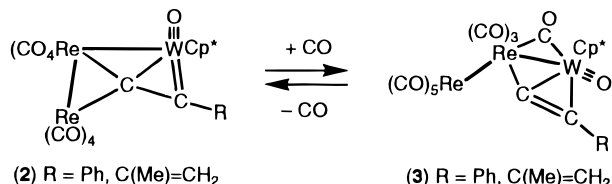
identified as acetylide complex $\text{Cp}^*\text{WRe}_2(\mu\text{-O})(\mu\text{-H})_2[\mu\text{-CCC}(\text{Me})=\text{CH}_2](\text{CO})_6$ (**5b**, 32%), alkenyl complex $\text{Cp}^*\text{W}(\text{O})\text{Re}_2[\mu\text{-CHCHC}(\text{Me})=\text{CH}_2](\text{CO})_8$ (**6b**, 15%), alkylidene complex $\text{Cp}^*\text{W}(\text{O})\text{Re}_2(\mu\text{-H})[\mu\text{-CHCH}_2\text{C}(\text{Me})=\text{CH}_2](\text{CO})_8$ (**7b**, 4%), and allenyl complex $\text{Cp}^*\text{WRe}_2(\mu\text{-O})[\mu\text{-CHCC}(\text{Me})_2](\text{CO})_7$ (**8**, 8%). The first three compounds were identified according to their IR and ^1H and ^{13}C NMR data, as their structures were analogous to the phenyl complexes **5a**, **6a**, and **7a** mentioned in the preceding section. The cluster **8** corresponds an unknown allenyl cluster, and its structure was further established crystallographically.

As indicated by the ORTEP diagram (Figure 6), the molecule consists of a WRe_2 triangular geometry in which each Re atom is coordinated by three terminal CO ligands and the seventh CO ligand is bridging across a W-Re bond. The bridging oxo ligand spans the $\text{W-Re}(2)$ bond and falls on the extension of the WRe_2 plane. The allenyl ligand adopts a normal $\mu_3\text{-}\eta^1, \eta^2, \eta^2\text{-mode}^{25}$ with the $\text{C}_\alpha\text{-C}_\beta$ vector parallel to the $\text{W-Re}(1)$ edge. The C_3 backbone of this allenyl ligand is bent, with the $\text{C}(8)\text{-C}(9)\text{-C}(10)$ angle of 139(1)° being comparable to those reported (138(2)–152(1)°) for the trinuclear allenyl complexes.²⁶ The M-C_γ distance ($\text{Re}(2)\text{-C}(10) = 2.49(1)$ Å) is significantly longer than the other M-C_α and M-C_β bonds within the molecule (2.09(1)–2.26(1) Å). Such a large deviation in M-C distances suggests the existence of a weakened bonding interaction between the Re atom and the $\text{C}_\beta\text{-C}_\gamma$ fragment. The short $\text{C}(9)\text{-C}(10)$ distance of 1.34(2) Å, which is close to that of the $\text{C}=\text{C}$ double bond in free ethylene (1.34 Å), conforms with this observation. This elongation of the M-C_γ bond in the allenyl cluster **8** has been seen in the related allenylidene cluster $\text{Cp}^*\text{WRe}_2(\mu\text{-OMe})[\text{CCC}(\text{Me})_2](\text{CO})_8$ ⁵ but has not been reported for the

(25) (a) Wojcicki, A.; Shuchart, C. E. *Coord. Chem. Rev.* **1990**, 105, 35. (b) Wojcicki, A. *J. Cluster Sci.* **1993**, 4, 59.

(26) (a) Shuchart, C. E.; Wojcicki, A.; Calligaris, M.; Faleschini, P.; Nardin, G. *Organometallics* **1994**, 13, 1999. (b) Nucciarone, D.; MacLaughlin, S. A.; Taylor, N. J.; Carty, A. J. *Organometallics* **1988**, 7, 106. (c) Suades, J.; Dahan, F.; Mathieu, R. *Organometallics* **1988**, 7, 47. (d) Gervasio, G.; Osella, D.; Valle, M. *Inorg. Chem.* **1976**, 15, 1221.

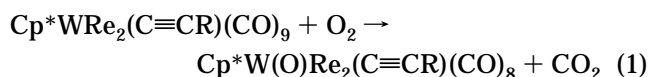
Scheme 2



allenyl cluster.²⁷ Finally, the ¹³C NMR signals of the allenyl ligand appears at δ 165.0 (C _{β}), 136.0 (J_{WC} = 97 Hz, C _{α}), and 66.0 (C _{γ}), which fall in the chemical shift range expected for the related allenyl clusters.

Discussion

Oxidation of the acetylide complexes **1** with oxygen produced the corresponding oxo cluster compounds **2**. After the elimination of a CO ligand as CO₂, the framework opens up to give an L-shaped geometry. The possible reaction stoichiometry is shown in eq 1: In

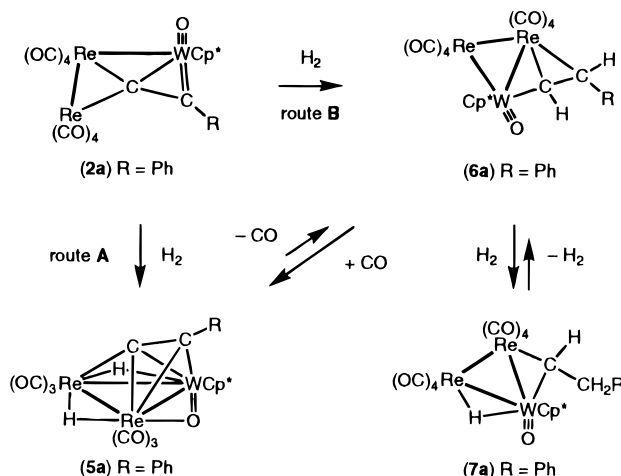


addition, replacing oxygen with other mild oxidant, e.g. nitrous oxide, increases the yields by 5–10%. Substantial decomposition was noted when the reaction was carried out in refluxing toluene at 110 °C. The successful isolation of **2** in high yields demonstrates the potential of using oxygen or nitrous oxide as a source in generation of metal complexes and cluster compounds containing oxo ligands.²⁸ This method complements the various oxidative decarbonylation strategies using iodosylbenzene,²⁹ hydrogen peroxide,³⁰ dioxirane,³¹ and air oxidation.³²

The acetylide ligand in **2** adopts a novel $\mu_3\text{-}\eta^1, \eta^1, \eta^2$ -mode with C _{α} connected to all three metal atoms and C _{β} coordinated to a W atom via a double bond. No such bonding mode has ever been reported in the system of acetylide clusters.³³ We believe that this mode has some connection with the electron deficiency of the Cp*W(O) fragment, induced by the coordination of the electronegative oxo ligand.

Upon heating under CO atmosphere, complexes **2** absorb one CO ligand, forming the clusters **4** with one Re(CO)₄ unit converting to the Re(CO)₅ unit and with the acetylide ligand changing to the edge-bridging mode (Scheme 2). As a result, the terminal Re(CO)₅ unit is no longer connected to the acetylide ligand. The free rotation around the Re–Re bond becomes attainable under this circumstance. The observation of a broad ¹³C NMR signal at δ 190.9 for **4a** and δ 191.0 for **4b** at room temperature with a ratio corresponding to four CO ligands, which are assigned to the equatorial CO ligands

Scheme 3



on the terminal Re(CO)₅ unit, support the existence of such dynamic motion in solution. Pyrolysis of complexes **4** in the absence of CO leads to the regeneration of the corresponding complexes **2** in high yields. These experiments suggest that the interconversions between **2** and **4** are fully reversible.

In contrast to the simplicity of CO addition, hydrogenation of **2a** afforded a mixture of three compounds **5a**, **6a**, and **7a** (Scheme 3). Upon increasing the temperature to 110 °C in toluene, the yield of **5a** dropped substantially while the total yields for **6a** and **7a** increased only moderately. These experiments suggest that **5a** is unstable while **6a** and **7a** are thermodynamically more favorable.

In principle, the transformation from **2** to **5**, **6**, and **7** can be understood within the framework of two competing pathways. The key step for the first pathway (route A of Scheme 2) involves the removal of at least one CO prior to the initial coordination of H₂ or immediately after the addition of H₂. The formation of **5** requires the loss of a second CO ligand, which leads to the formation of the triangular metal framework. Interestingly, when **5a** was treated with CO in refluxing dichloromethane solution, it slowly gave **6a** in low yield, together with a small amount of **2a** by loss of a H₂ molecule. This reactivity pattern reveals the delicate balance of the dehydrogenation reaction vs the hydride migration to the acetylide ligand.

On the other hand, the formation of alkenyl complexes **6** and alkylidene complexes **7** involves the direct addition of H₂ without the prior elimination of CO ligand (route B). This postulation is supported by the fact that complexes **2**, **6**, and **7** own the same number of CO ligands. It is possible that H₂ first coordinates to the WRe₂ framework of **2** to afford a dihydride intermediate with a hypothetical formula Cp*W(O)Re₂(μ -H)₂(CCR)(CO)₈, which then converts to the alkenyl complexes **6** by transferring both hydrides to the acetylide. The prospect involving the direct addition of H₂ over the acetylide is eliminated because of the *trans* configuration observed for the alkenyl ligand.

Complexes **6** then react further with another H₂ molecule to form the alkylidene ligand in **7**. The addition of the second H₂ molecule is highly regioselective because of the isolation of only one alkylidene isomer. This proposed sequential addition of H₂ is further supported by the D₂ labeling experiments. Treatment of **6a** or **6b** with D₂ afforded the labeled

(27) (a) Young, G. H.; Raphael, M. V.; Wojcicki, A.; Calligaris, M.; Nardin, G.; Bresciani-Pahor, N. *Organometallics* **1991**, *10*, 1934. (b) Doherty, S.; Corrigan, J. F.; Carty, A. J.; Sappa, E. *Adv. Organomet. Chem.* **1995**, *37*, 39.

(28) Bottomley, F.; Chen, J. *Organometallics* **1992**, *11*, 3404.

(29) Kim, J.-H.; Hong, E.; Kim, J.; Do, Y. *Inorg. Chem.* **1996**, *35*, 5112.

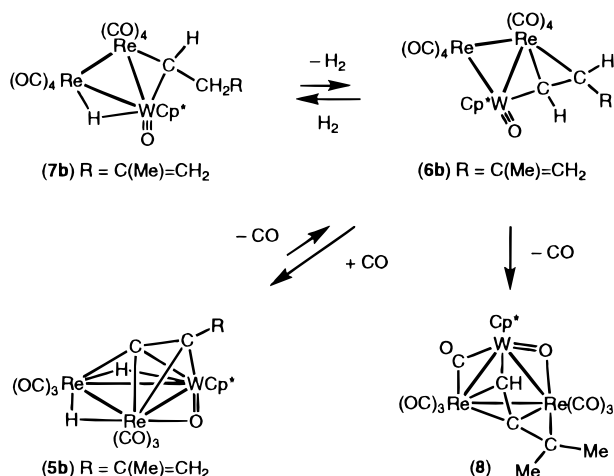
(30) (a) Bottomley, F.; Boyle, P. D.; Chen, J. *Organometallics* **1994**, *13*, 370. (b) Thiel, W. R.; Fischer, R. W.; Herrmann, W. A. *J. Organomet. Chem.* **1993**, *459*, C9.

(31) Bolowiec, S.; Kochi, J. K. *Inorg. Chem.* **1991**, *30*, 1215.

(32) Alt, H. G.; Hayen, H. I.; Rodgers, R. D. *J. Chem. Soc., Chem. Commun.* **1987**, 1795.

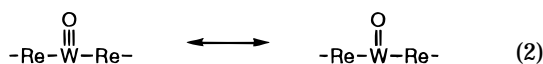
(33) (a) Sappa, E.; Tiripicchio, A.; Braunstein, P. *Chem. Rev.* **1983**, *83*, 203. (b) Sappa, E. *J. Cluster Sci.* **1994**, *5*, 211. (c) Jeannin, Y. *Transition Met. Chem. (London)* **1993**, *18*, 122.

Scheme 4



complexes **7**, Cp*W(O)Re₂(μ-D)(μ-CHCHDR)(CO)₈ (R = Ph or C(Me)=CH₂) in which the deuterium atoms selectively replaced the hydride and one methylene hydrogen of the alkylidene ligand.

The unsaturation required for the activation of H₂ on the WRe₂O core in both **2** and **6** may be generated through (i) a reversible cleavage of the metal–metal bond or (ii) a reversible two-electron reduction in donor capability of the oxo ligand, as indicated in eq 2. The



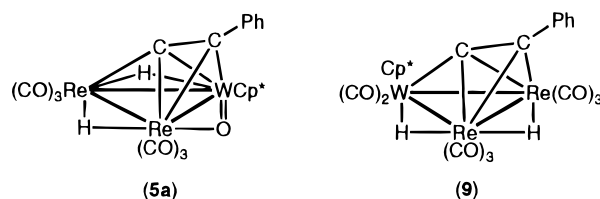
reversible conversion between complexes **2** and **4** is a precedent to process i. Process ii has been proposed to occur, in an attempt to account for the greater affinity of the oxo–alkylidene cluster CpWOs₃(μ-O)(μ₃-CH₂Tol)(CO)₉ with various reagents including CO, H₂, phosphines, alkynes, and alkenes.³⁴ We cannot eliminate either possibility based on our present experimental data. In addition, thermolysis of **7a** or **6a** under N₂ generates a mixture of **7a**, **6a**, and **5a** or a mixture of **6a**, **5a**, and **2a**, respectively. These experiments clearly demonstrate that the dehydrogenation sequence, a reverse transformation from **7** to **6** and then a mixture of **2** and **5**, is feasible and involves the same activating process.

For the hydrogenation of the vinylacetylide complex **2b**, in addition to the expected mixture of **5b**, **6b**, and **7b**, we observed the formation of the allenyl cluster compound **8** in low yield (Scheme 4). The relationship between compounds **5**, **6**, **7**, and **8** was established on the basis of the reaction stoichiometry and their reactivities. According to our previous delineation, two possible reaction pathways can be proposed to account for the production of **8**. The first one involves a concerted addition of two hydrogen atoms to the C_α

position and the remote methylene group of the vinylacetylide ligand C≡CC(Me)=CH₂ in **2b**. Alternatively, a concerted or a transition metal mediated 1,3-H-migration from the C_β position of the CH=CHC(Me)=CH₂ ligand in **6b** to the methylene site, along with the elimination of CO, would give the same product **8**. We favor the second mechanism, as thermolysis of both allenyl complex **6b** and alkylidene complex **7b** have all afforded the allenyl complex **8** in moderate yields. Finally, this transformation from vinylalkenyl to allenyl via the 1,3-H-migration is related conceptually to the conversion of an alkyne (HCCR) to a vinylidene (CCHR) on trinuclear clusters via a 1,2-H-shift.³⁵

Conclusion

In summary, we present here the facile synthesis of WRe₂ clusters containing the oxo ligand and the subsequent conversion of the ligated acetylide to allenyl, alkylidene, and allenyl upon treatment with hydrogen and the thermally induced isomerization. The oxo ligand in these complexes adopts either the terminal or the asymmetrical, doubly-bridging mode. The precise role of the oxo ligand in the conversions between **2** ↔ **4** and **2** → **6** → **7** remains in doubt, although we have demonstrated that this reaction pattern is suppressed in the absence of an oxo ligand. Thus, the parent complex **1** failed to react with CO. Carbonylation of the hydrido–acetylide cluster Cp*WRe₂(μ-H)₂(CCPh)(CO)₈ (**9**),⁵ which is related to **5a** by formally replacing the bridging oxo ligand with two CO ligands, produced only elimination of H₂. Whether the contribution of the oxo



ligand via its high electronegativity and its capability to shuttle between a four- and six-electron donor^{33,36} and to adopt various bonding modes are the key factors to promote such reactions awaits the results of continuing explorations.

Acknowledgment. We thank the National Science Council of the Republic of China for financial support (Grant No. NSC 85-2113-M007-008).

Supporting Information Available: Tables of atomic coordinates and anisotropic thermal parameters for complexes **4a**, **6a**, **7a**, and **8** (16 pages). Ordering information is given on any current masthead page.

OM9609426

(34) (a) Chi, Y.; Shapley, J. R.; Churchill, M. R.; Fetting, J. C. *J. Organomet. Chem.* **1989**, *372*, 273. (b) Park, J. T.; Chi, Y.; Shapley, J. R.; Churchill, M. R.; Ziller, J. W. *Organometallics* **1994**, *13*, 813. (c) Churchill, M. R.; Bueno, C.; Park, J. T.; Shapley, J. R. *Inorg. Chem.* **1984**, *23*, 1017.

(35) (a) Cooksey, C. J.; Deeming, A. J.; Rothwell, I. P. *J. Chem. Soc., Dalton Trans.* **1981**, 1718. (b) Vahrenkamp, H.; Roland, E. *J. Mol. Catal.* **1983**, *21*, 233. (c) Bantel, H.; Powell, A. K.; Vahrenkamp, H. *Chem. Ber.* **1990**, *123*, 1607.

(36) (a) Shapley, J. R.; Park, J. T.; Churchill, M. R.; Ziller, J. W.; Beanan, L. R. *J. Am. Chem. Soc.* **1984**, *106*, 1144. (b) Chi, Y.; Hwang, L.-S.; Lee, G.-H.; Peng, S.-M. *J. Chem. Soc., Chem. Commun.* **1988**, 1456.